PHYSICAL REVIEW A VOLUME 20, NUMBER 5 NOVEMBER 1979

Transition probabilities and Stark-broadening parameters of neutral and singly ionized lead

Myron H. Miller
Department of Mechanical Engineering, U.S. Naval Academy, Annapolis, Maryland 21401

Roger D. Bengtson
Department of Physics, University of Texas at Austin, Austin, Texas 78712

John M. Lindsay
MITRE Corporation, 1820 Dolley Madison Boulevard, McLean, Virginia 22101
(Received 18 June 1979)

Strengths and Stark widths of the prominent visible Pb I and Pb II lines are measured in emission by means of a gas-driven shock tube. Absolute ionic line strengths for $7s$-$7p$ and $7p$-$7d$ arrays conform well to quantum-mechanical sum rules and agree with theoretical predictions, but $6d$-$5f$ results differ markedly from central-field approximations. Neutral-line strengths agree satisfactorily with available comparison data. Semiempirical theory predicts the widths of Pb II lines with characteristic reliability of better than 25%.

INTRODUCTION

The suitability of relativistic and nonrelativistic treatments of heavy-element gf values has recently been examined theoretically.[1] The single active electron in the visible Pb II transitions is moderately excited,[2] so that computational complications due to core (closed s-shell) penetration are averted. Mixing between the well-separated configurations[2] is also unlikely. Integrals of radial wave functions are not susceptible to cancellation effects.[3] Because of this simple structure, experimental line-strength data affords a particularly direct test of theoretical models applied to heavy elements. Similarly, linewidth measurements test line-broadening models[4] in an uncustomarily high-z domain. The persistent astrophysical interest[5] in the stellar abundance of lead notwithstanding, no quantitative strength or shape data have heretofore been reported[6] for these prominent lines accessible to ground-based observers.

Several features facilitate study of Pb II lines in thermal light sources. Their brightness in 1-eV plasmas, coupled with a marked Stark-effect broadening, yield desirable signal-to-noise ratios without appreciable radiative trapping in line cores. The dominant $7s$-$7p$, $7p$-$7d$, and $5d$-$5f$ transition arrays lie completely in the visible where detectors are readily calibrated and have good sensitivity. Recording of complete arrays permits line strengths to be tested for conformity with one-electron[7] (f sum) and J-file[8] sum rules. Blending between the Pb II lines or interference from Pb I lines is not consequential. Although the primary intent of this work is to determine the absolute strengths and Stark widths of the prominent visible Pb II lines, relative strengths of visible and near-ultraviolet lines of Pb I are also obtained as a complement to lifetimes reported in the literature.[9-13]

EXPERIMENTAL

The apparatus and methods used on lead are similar to those we employed on earlier line strength and width studies of the group-IV spectra of Si,[14] Ge,[15,16] and Sn[17] and several other species.[18,19] Accordingly, description of the light source, instrumentation, and data reduction will be given in little detail except for factors unique to the excitation, recording, and analysis of Pb I and Pb II lines. At the outset, we review the generic problems of time-resolved absolute photographic photometry and how our experimental design deals with the major sources of systematic error.

The customary sources of bias in shock-tube line-strength determinations are twofold. Error in absolute emitter densities can arise either from the critical sensitivities of excited-state populations to uncertainty in source temperature or from undetected loss of subject element prior to shock heating. Secondly, there is the well-known difficulty in maintaining reliable absolute and relative calibration in fast spectroscopic emulsions.

Our program to minimize repeatable error includes several steps.

(i) Absolute ionic A values involve trans-species relative line-strength measurements, using H_β as a reference A value. That is, the subject transition probability A is computed from

$$A = A_{H_\beta} \frac{\lambda}{\lambda H_\beta} \frac{N_{H_\beta}}{N} \frac{I}{I_{H_\beta}},$$

where N, λ, and I are the emitting-state population density, wavelength, and integrated line intensity, respectively. The ratio of integrated intensities I/I_{H_β} depends on relative detector response and calibration. Generally, the H_β and Pb II line peak brightnesses are similar, so that the comparison I/I_{H_β} is between signals of comparable strength and signal-to-noise ratio. The population density ratio N_{H_β}/N has only a slight dependence on measured temperature, as shown in Fig. 1. Because the ratio of lead and hydrogen are fixed stoichiometrically by the test gas $Pb(C_2H_5)_2$, and there is no demixing of plasma constituents in the shock tube during the short test time, only the mild uncertainty shown in Fig. 1 is introduced by the possibility of unspecified tetraethyl lead absorption on the tube walls prior to shock heating.

(ii) Because the A value of Pb I for $\lambda = 4057.8$ Å has been deduced from precise lifetime data, 9–13 neutral-lead transition probabilities are measured relative to this line. Ratios of excited-state population densities depend only weakly on possible error in measured temperature. Some reabsorption in the thin laminar boundary layers cannot be ruled out—but since the visible Pb I lines are several eV removed from ground, it is expected to be slight, and indeed is not detectable when experimental Pb I profiles are fitted to appropriate Voigt shapes.[20]

(iii) Stark-broadening parameters similarly depend on relative rather than absolute data. Since plasma electron densities N_e are obtained from the width of H_β profiles[21] recorded simultaneously with the lead profiles, the ratio of lead-line Stark widths to electron density depend primarily on the ratio of relative widths $w_{Pb}/(w_{H_\beta})^{2/3}$, the H_β half-width scaling as the two-thirds power of plasma electron density. Any systematic error in an emulsion response curve therefore propagates as the one-third power into the measured broadening parameter. Deconvolution, often a source of systematic error,[22] is not troublesome here due to the lead lines being severalfold wider than instrumental profiles, as illustrated by the simultaneously recorded lead and fiduciary profiles shown in Fig. 2.

(iv) Absolute photometric data, used to determine plasma temperature and to make routine compensation for finite optical depths, is recorded photoelectrically—thus circumventing the difficulty of maintaining absolute photographic calibration.

(v) Most important variables are measured redundantly. The lead spectra are recorded simultaneously on two spectrographs; one obtains well-resolved (1/3-Å typical resolution) profiles, which are fitted to appropriate Voigt shapes and the other with an integrating 4 Å instrumental bandpass from which partially integrated profiles are read with a planimeter. The two instruments use different emulsions and are individually calibrated. Temperatures are measured by two or three techniques in each experiment. Plasma pressure is also measured, so that our electron density measurements overdetermine the thermodynamic state of the light source.

(vi) Plasma temperatures $[(10.3\text{–}12.4)\times 10^4\,°K]$, electron densities $[(5\text{–}13)\times 10^{16}\,cm^{-3}]$ and lead–additive concentrations (0.25–0.6% molal) were deliberately varied in an attempt to uncover any bias which might depend on plasma brightness, linewidths, or signal-to-noise or line-to-background ratios.

The shock tube is of conventional cold-driver design,[23] with inside dimensions of $7.1\times 9.7\,cm^2$. The spectroscopic light source is the quasistationary plasma behind first- and multiply-reflected shocks. Prior testing showed these plasmas to be free of repeatable inhomogeneities (except for thin laminar boundary layers) and to conform to assumptions of local thermal equilibrium.[24]

Viewed a few centimeters off the tube's end wall, the spectroscopic plasma's steady-state test times were 40–200 μs, depending on filling pressures. Driver gas was 1000–1200 psi (absolute) of ambient-temperature hydrogen. The test gas was 6–300 Torr of a neon carrier containing 0.25–0.6% molal concentrations of tetraethyl lead. Initial test gas pressure and composition was adjusted by trial to give desirable photometric signal strengths (good signal-to-noise ratios without appreciable radiative trapping).

Precautions were taken to avoid demixing during test gas mixing and metering operations, but these did not insure against undetected partial absorption of the small $Pb(C_2H_5)_2$ concentrations on the shock-tube walls prior to firing. As shown in Fig. 1, at a typical plasma pressure (2×10^7 dyn cm^{-2}), the ratio of ionic lead line to H_β population density is quite insensitive even to factor-of-3 hypothetical losses in tetraethyl lead. Discrepancies between measured electron densities and electron densities deduced from temperature and pressure data would disclose $Pb(C_2H_5)_2$ loss of significant magnitude.

Instrumentation for time-resolved photometry includes 1-m (1700 Å at 1/3-Å resolution) and 3/4-m (3000 Å at 4-Å resolution) spectrometers for photographically recording lead and Balmer profiles. A beam splitter permitted these two instruments to view the plasma along a common optical axis and to share a single fast shutter.[25] Several monochromaters with multichannel (line-

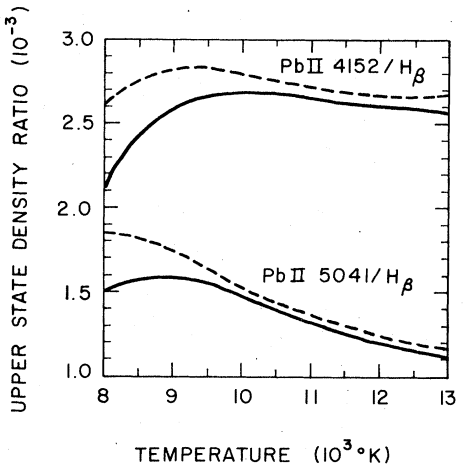

FIG. 1. Ratios of excited-state number densities for PbII 4152/H_β and PbII 5041/H_β, as functions of temperature. Plasma pressure is 2.0×10^7 dyn cm^{-2}. The curves representing test gas compositions (dashed line) 0.45% Pb$(C_2H_5)_2$ and (solid line) 0.15% Pb$(C_2H_5)_2$ differ only slightly between 10 000 °K and 12 000 °K, the usual experimental range.

plus-nearby background) photoelectric recording measured the absolute brightness of H_β, prominent neon red lines and the continuum. These data were used to find plasma temperature and to reduce the lead and H_β (photographic) profiles to their appearance in the optically thin limit.[26] A monochromator centered on optically thick H_α was briefly backlighted by a flashlamp to obtain plasma temperature by the line-reversal method.[27] A pair of quartz transducers recorded the plasma pressure. Calibration of the spectrographs was carried out with a well-regulated carbon arc[28] and tested for reciprocity failure with a variety of continuous and discrete transient light sources.[18]

In every run, the excitation temperatures from the integrated energy in 5852-Å NeI and H_β (excitation potentials of 18.6 and 12.7 eV, respectively) and from line-reversal (blackbody temperature) were each determined with estimated accuracy of typically ±5%. In most instances, results of the three measurements agreed within these tolerances, and were in conformity with the temperature deduced from inverting electron density via the H_β halfwidth and pressure data.

By fitting (red-and-blue wing-averaged) H_β profiles to theoretical shapes,[21] electron densities could be found with an estimated accuracy of ±(15–20)% per exposure. Photometric quality control consisted of rejecting exposures whose specular density did not register on the quasilinear portion of the emulsion γ curves, or for which exposures spanned non-stead-state plasma conditions (ascertained by photoelectric monitors in the spectrograph's focal planes) or when peak optical depths were excessive. This program of culling led to rejection of data from approximately one-half of the experimental runs.

For the stronger Pb II lines, widths determined by nine-point fitting to dimensionless Voight profiles were estimated to be generally reliable to 15–20% prior to deconvolution. After correction for slit-induced and Doppler broadening, reliability of the Lorentzian width components was of order 20–25%. The Stark-broadening parameters w(= Lorenzian width at half intensity)/N_e, therefore contain about 30–35% random error per experiment. The number of independent determinations varied with a line's strength and wavelength, but ten to twenty were the rule.

From a spectrogram of usual quality, the ratio of Pb II to H_β line strengths could be measured with 25% precision, photographic noise from the grainy emulsions being the chief source of jitter, as can be inferred from Fig. 2. Relative integrated intensities measured by the independently calibrated line-integrating and line-resolving spectrographs agreed well, as shown in Fig. 3. It is noted that the depicted ratios of line intensities covered a broad range of brightnesses, linewidths, and line-to-background ratios. Optical depth corrections were most substantial for 5608.8-Å PbII. When peak optical depths for this line exceeded 0.5, the data was discarded. The neutral lead lines gave poorer signal-to-noise ratios than ionic ones for most plasma conditions. On this account,

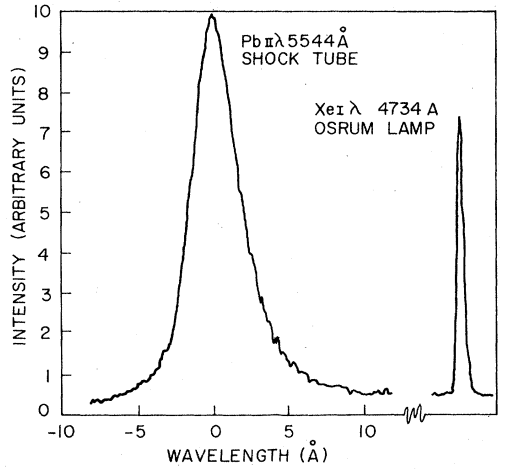

FIG. 2. Relative intensity vs wavelength plots of two lines recorded on the same photographic exposure. The 5544-Å PbII profile is obtained from a shock-tube plasma at $N_e = 8.6\times10^{16}$ cm^{-3} and $T = 11\,900$ °K. The 4731-Å XeI line is superimposed on the shock-tube spectrum using an Osrum lamp.

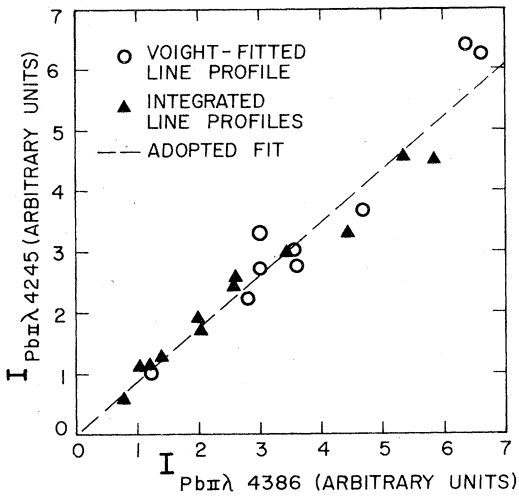

FIG. 3. Comparison of integrated line intensities, $\int I(\lambda)d\lambda$, of 4245-Å Pb II vs 4386-Å Pb II. These data were recorded by two different photographic methods. The open points represent measurements obtained from a one-meter spectrograph whose $\frac{1}{3}$-Å instrumental width is small compared to plasma Pb II linewidths. Fitting the experimental profiles to appropriate Voigt shapes discriminated line wings from background The solid triangles represent lines recorded on a $\frac{3}{4}$-m spectrograph whose slit opening partially integrated a line's intensity: the partially integrated profiles were read with a planimeter. The two instruments used different emulsions and were independently calibrated.

and also because of an allowance for undetected reabsorption in the boundary layers, A values for Pb I are less reliable than simultaneously measured Pb II lines. Between eight and twenty-four strength determinations were obtained, depending on a line's brightness and its proximity to H_β.

In a minority of the runs, 5052-Å C I attained useful brightness. Since the strength of this line is regarded as being approximately known,[3,18,29] we measured its A value as a control. Results agreed with the literature transition probabilities and halfwidths.[19,22]

RESULTS AND DISCUSSION

Absolute transition probabilities of Pb II are given in Table I. Uncertainties quoted for shock-tube data combine statistical analysis of random error (2σ) with 90% tolerance estimates of possible bias. Aside from 5042.5-Å Pb II being marginally affected by blending with weak 5041.7-Å C I, differences in accuracy between various lines are photometric in origin. Highest reliability corresponds to superior signal-to-noise ratios per exposure, and to a larger number (typically 18–24) of experimental runs registering within our emulsion's dynamic response range. No fewer than eight exposures were obtained for results denoted as "C" accuracy.

TABLE I. Absolute transition probabilities of singly-ionized lead ($10^8 s^{-1}$).

Wavelength (Å)	Transition[a]	This work[b]	Trukhan *et al.*[c] (pulsed discharge)	Brown[d] (shock tube)	Migdalek[e] (relativistic)	Coulomb approximation[f]
4245.1	$6d\,^2D_{5/2}-5f\,^2F^o_{7/2}$	0.29*B*	1.28[g]	>4.0		2.9
4386.4	$6d\,^2D_{3/2}-5f\,^2F^o_{5/2}$	0.44*B*		>8.6		2.6
5544.6	$7p\,^2P^o_{3/2}-7d\,^2D_{5/2}$	1.04*A*				1.00
5042.5	$7p\,^2P^o_{1/2}-7d\,^2D_{3/2}$	0.77*A*				0.89
5608.8	$7s\,^2S_{1/2}-7p\,^2P^o_{3/2}$	1.24*B*			1.25	1.00
6660.0	$7s\,^2S_{1/2}-7p\,^2P^o_{1/2}$	0.62*B*			0.74	0.68
5372.1	$6s6p\,^4P_{5/2}-6s\,^25f^2F^o_{7/2}$	1.28*A*				...
3785.9	$6s6p\,^4P_{3/2}-6s\,^25f^2F^o_{5/2}$	0.033*C*				...
4152.8	$7p\,^2P^o_{3/2}-9s\,^2S_{1/2}$	0.24*C*			0.30	0.19

[a] Classification from C. E. Moore (Ref. 30).
[b] Estimated uncertainty: $25\% \leq A \leq 30\%$, $30\% \leq B \leq 35\%$, $35\% \leq C \leq 45\%$.
[c] Reference 31.
[d] Reference 33.
[e] Reference 1.
[f] Integrals of radial wave functions from tables of Oertel and Shomo (Ref. 34) used with LS coupling.
[g] If a lifetime-derived A value for Pb I 4168.0 is used instead of the Corliss and Bozman (Ref. 32) value for normalization, the Pb II λ4245 A value becomes 4.0×10^8 s^{-1}.

Experimental comparison data are fragmentary. Trukhan, *et al.*[31] measured the line-strength ratio 4245.1-Å Pb II/4168.0-Å Pb I in a pulsed discharge and used the neutral-lead A value of Corliss and Bozman[32] for reference. Subsequently, a three-fold larger 4168.0-Å Pb II result was derived from lifetime measurements. Renormalizing to this later neutral-lead A value would scale the Trukhan, *et al.*[31] result to 4.0×10^8 sec^{-1}. Brown's[33] lower-limit determinations via a gas-driven shock tube are limited to two lines of a single multiplet.

Two sets of theoretical predictions are available: Migdalek's computations[1] incorporating relativistic and exchange effects, and the author's calculations based upon tabulated[34] scaled hydrogenic central-field integrals and LS coupling. All multiplets satisfy criteria[35] for optimal application of the Coulomb approximation.

Comparison of line strengths from these various sources poses a confusing picture of agreements and discordances. The most obvious feature of Table I is the satisfactory agreement of absolute shock-tube results with theory for all arrays except $6d$-$5f$. All the relativistic and two out of three Coulomb approximations fit the shock-tube data within experimental tolerance. On the average, the ratio of Coulomb approximations to shock-tube data is 1.01, with σ = 36%. Migdalek's[1] predictions appear consistently too large by about 19%, with an 18% scatter in the ratio of theory to experiment. A tendency has been noted elsewhere for similar relativistic calculations to moderately overestimate[17,36,37] experimental transition probabilities.

Confidence in the absolute shock-tube A values for leading ($7s$-$7p$ and $7p$-$7d$) transition arrays is reinforced by testing for conformity with the one-electron sum rules.[7] In Table II the array average-absorption oscillator strengths for all dipole-allowed radiative channels into and out of the $7p$ level are tallied for comparison with the expectation values of the Wigner-Kirkwood (WK) and Thomas-Reiche-Kuhn (TRK) sum rules. Shock-tube data, which account for the preponderance of both column's f sums, are augmented by refined theoretical predictions (Migdalek[1]) and asymptotic approximations.[7] Agreement with the WK sums for both the Σ_n ns-$7p$ and Σ_n $7p$-nd cases, and also the TRK (combined) sum, is well within experimental tolerance.

Misgivings over shock-tube absolute A values for $6d$-$5f$ transition array being an order of magnitude smaller than corresponding Coulomb approximations is heightened by the fact that the independent experiments of Trukhan[31] (if scaled to lifetime data for Pb I) and Brown[33] are in approximate agreement with theory. However, the good agreement between our ns-np, np-nd transition-array A values and both Coulomb approximations and quantum-mechanical sum rules, together with discrepancies between d-f findings and corresponding central-field predictions, has been a persistent feature of our work with other group-IV first

TABLE II. Array-average oscillator strengths for transitions involving $6s^2 7p$ of Pb II compared with f sum rules.

Initial configuration	$7P$	
Final configurations[a]	ns	nd
$n=6$	...	−0.14[c]
$n=7$	−0.53	0.73
$n=8$	0.31[b]	0.15[c]
$n=9$	0.03	0.06[c]
$n=10$	0.01[b]	0.03[d]
$n=11$ to ∞	0.01[d]	0.07[d]
Continuum	0.01[d]	0.21[d]
Partial sum	−0.16	1.11
WK sum-rule	≈−0.11	≈1.11
Sum	0.95	
TRK sum rule	≈1.00	

[a] Only dipole-LS-allowed transitions are taken into account.
[b] Relativistic calculations by Migdalek (Ref. 1).
[c] Coulomb approximations using tabulated integrals of radial wave functions by Oertel and Shomo.
[d] Scaled hydrogenic approximations via Bethe and Salpeter (Ref. 7).

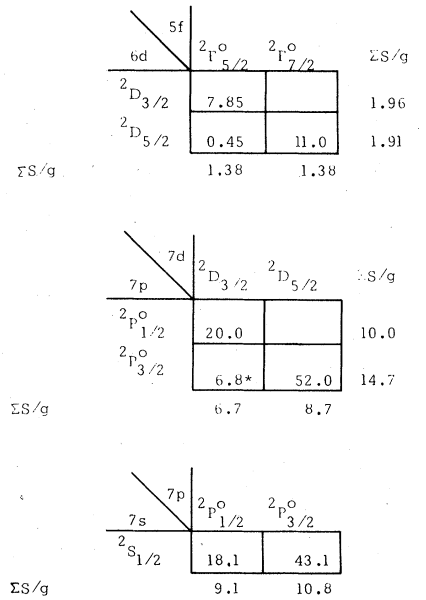

FIG. 4. Relative strengths within leading Pb II transition arrays examined for conformity with the J-file sum rule. Asterisk means predicted via LS coupling.

TABLE III. Comparison of measured and predicted oscillator strengths for leading d-f transition arrays of group-IV ions.

Ion	Transition array	n_i^*	n_k^*	Array[f] value Measured[a]	Theoretical[b]
Si II	$3d-4f$	2.89	3.94	0.49	0.90
Ge II	$4d-4f$	3.04	3.95	0.79	1.02
Sn II	$5d-4f$	3.07	3.91	0.69	1.21
Pb II	$6d-5f$	2.91	3.91	0.14	1.06

[a] Tabulated data is from present shock tybe (Ref. 15–17).

[b] Author's computation based on tabulated (Ref. 34) integrals of scaled hydrogenic wave functions.

ions. For Si II, Ge II, and Sn II, our absolute A values[37] satisfy the WK and TRK sum rules within estimated experimental error and agree with Coulomb approximations, but as Table III shows, measured d-f oscillator strengths are significantly smaller than their Coulomb approximation counterparts (which are nearly invariant in the sequence, reflecting the approximately constant effective principle quantum numbers).

If the discrepancies in d-f transition arrays are experimental in origin, one would suspect either failure of the light source to populate emitter levels in accordance with the Boltzmann statistics, or bias in our photometry. The first possibility is deemed unlikely because electron densities $[(5–13)\times10^{16}$ cm$^{-3}]$ are fully an order of magnitude greater than required to maintain local thermodynamic equilibrium.[38] Furthermore, effective principle quantum numbers of the ns, np, and nd levels giving rise to those transitions whose strengths do agree with theory, bracket those of the d-f levels in question. In view of the good agreement of ns-np and np-nd transition-array results and theory-sum rules, any bias in photometry would be of a relative rather than absolute nature. The shapes,

TABLE IV. Experimental lifetimes for states of Pb I. Relative A values of Corliss and Bozman were used to estimate branching of λ 2053 and λ 5201 with respect to λ 3672 according to $\tau=(A_{2883}+A_{3639}+A_{4057})^{-1}$.

$6p7s\ ^3P_1$	5.75 ± 4%	Saloman and Happer[a]
	5.58 ± 13%	de Zafra and Marshall[b]
	6.05 ± 5%	Cunningham and Link[c]
	5.6 ± 9%	Novik *et al.*[d]
$6p8s\ ^3P_1$	12.9 ± 11%	Saloman[e]

[a] Reference 9.
[b] Reference 10.
[c] Reference 12.
[d] Reference 11.
[e] Reference 13.

TABLE V. Transition probabilities for neutral lead (10^8s^{-1}) normalized to lifetime-derived A value[a] of λ 4057.8 Å.

Wavelength (Å)	Transition	This work[b] shock tube	Corliss and Bozman[c] free arc	Lotrian *et al.*[d] hollow cathode	Brown[e] shock tube	Khoklov[f] controlled arc	Penkin and Slavenas[g] controlled arc	Lambert[h] theory (STF)	Lawrence theory (STF)	Migdalek[i] theory IC	*ij*
3572.8	$6p^2(3/2,3/2)_2$-$6p7s(3/2,1/2)_1$	1.78*B*	1.28	1.09		1.48			2.12	1.77	1.45
3639.6	$6p^2(3/2,1/2)_1$-$6p7s(1/2,1/2)_1$	0.34*A*	0.13	0.37	0.21	0.25	0.32	0.30	0.34	0.27	0.27
3671.5	$6p^2(3/2,3/2)_2$-$6p8s(1/2,1/2)_1$	0.53*B*	0.39	0.49							
3683.5	$6p^2(3/2,1/2)_1$-$6p7s(1/2,1/2)_0$	1.48*A*	0.99	1.68	1.05	1.25	1.68	1.61	1.77	1.68	1.59
3739.9	$6p^2(3/2,3/2)_2$-$6p7s(3/2,1/2)_2$	1.08*B*	2.27	0.81		1.25		1.29	0.56	0.57	0.75
4019.6	$6p^2(3/2,3/2)_2$-$6p6d(1/2,5/2)_3$	0.12*A*	0.10	0.04							
4057.8	$6p^2(3/2,1/2)_2$-$6p7s(1/2,1/2)_1$	0.99_{ref}	0.99	0.99	0.99	0.99	0.99	0.99	0.99	0.99	0.99
4062.1	$6p^2(3/2,3/2)_2$-$6p6d(1/2,3/2)_1$	0.29*B*	0.35	1.02							
4168.0	$6p^2(3/2,3/2)_2$-$6p6d(1/2,5/2)_2$	0.06*B*	0.04	0.013							

[a] References 10–13.
[b] Accuracy: $30\% \leqslant A \leqslant 40\% \leqslant B \leqslant 60\%$.
[c] Reference 32.
[d] Reference 39.
[e] Reference 33.
[f] Reference 40.
[g] Reference 41.
[h] Reference 42.
[i] Reference 44.

TABLE VI. Stark-effect broadening of selected Pb II and Pb I lines.

Wavelength (Å)	Transition	Range of N_e (10^{16} cm^{-3})	Full-width at half intensity[a,b]
Pb			
4245.1	$6d\ ^2D_{5/2} - 5f\ ^2F^o_{7/2}$	5–13	1.69*A*
4386.4	$6d\ ^2D_{3/2} - 5f\ ^2F^o_{5/2}$	5–13	1.72*A*
5544.6	$7p\ ^2P^o_{3/2} - 7d\ ^2D^o_{5/2}$	8–11.5	3.60*A*
5042.5	$7p\ ^2P^o_{1/2} - 7d\ ^2D_{3/2}$	8–11.5	3.84*A*
5608.8	$7s\ ^2S_{1/2} - 7p\ ^2P^o_{3/2}$	8–11.5	1.96*C*
5372.1	$6s5p^2\ ^4P_{5/2} - 6s\ ^25f\ ^2F^o_{7/2}$	8–11.5	2.27*A*
4152.8	$7p\ ^2P^o_{3/2} - 9s\ ^2S_{1/2}$	10–11.5	2.34*C*
Pb I			
4057.8	$6p\ ^2(3/2,1/2)_2 - 6p7s(1/2,1/2)_1$	5–13	0.62*C*

[a] Estimated accuracy: $15\% \leq A \leq 20\% \leq B \leq 25\% \leq C \leq 40\%$.
[b] Results are for $N_e = 10^{17}$ cm^{-3}, $T = 11\,600°K \pm 1000°K$.

brightnesses, and wavelengths of the *d-f* lines are not unlike those for simultaneously recorded *ns-np* or *np-nd* lines—so that the photometric signals are not inherently different. The consistency (shown in Fig. 3) between relative line strengths independently recorded over a wide range of plasma brightnesses (and line-to-background ratios) also argues against a bias relative photographic photometry. Finally, we note that our intramultiplet relative line strengths for $6d$-$5f$, as well as $7s$-$7p$ and $7p$-$7d$, are in conformity with the *J*-file sum rules[8] as shown in Fig. 4.

Before turning to Pb I results, we comment on another curious result in Table I; namely, that the largest measured *A* value of Pb II results from a spin-flip transition.

Although our experimental conditions were deliberately tailored to enhance the Pb II spectrum, the dominant Pb I lines (3500 Å $< \lambda <$ 4200 Å) attained useful brightness in most runs. Radiative lifetimes for some Pb I states have been measured by the variety of techniques shown in Table IV. The excellent convergence of these data establish an absolute *A* value scale with far superior reliability than is possible with a thermal light source such as the shock tube. Therefore, we measure relative Pb I line strengths and normalize to the lifetime-derived *A* value of 4057.8-Å Pb I. The rationale for this work is twofold; firstly, it extends results of lifetime studies to considerably more transitions, and, secondly, it provides independent branching-ratio data which can be used to refine the transformation of lifetimes to *A* values.

Shock tube and comparison *A* values for Pb I, normalized to 4057.8-Å Pb I, are given in Table V. Estimated errors include an allowance for the uncertainty in the lifetime-derived data, but are due mainly to observed random and possible systematic error in relative photometry and reabsorption in laminar boundary layers.

The most extensive comparisons are from the Corliss Bozman (CB) reduction of Meggers's free-burning arc data, and from hollow cathode studies of Lotrian *et al.*[39] Agreement of CB with present results is spotty, ranging from ±20% to a factor of 3. For five Pb I lines measured by Lotrian *et al.*[39] with an "optical" electron in the upper state, results agree with shock-tube measurements. However the relative *A* values from upper *d* electrons show large discrepancies, suggesting a nonthermal population in the low electron density hollow cathode discharge. The three values from Brown's[33] shock-tube work, falling between the CB and present results, do not help to discriminate the more reliable set. The controlled-arc experiments of Khoklov[40] and of Penkin and Slavenas[41] both agree with present results to within either the estimated shock-tube error or the error than can be inferred from the differences between the two controlled-arc experiments. Results from these more refined arcs do not agree with the CB data to better than from 25% to a factor of 2.

Likewise, two independent sets of theoretical predictions are in markedly closer agreement with present results than with those of CB. With one exception Pb I λ 3739.9 Å), the results of Lambert *et al.*[42] (scaled-Thomas-Fermi with intermediate coupling) and Lawrence[43] (scaled-Thomas-Fermi

TABLE VII. Comparison of group-IV ionic-line Stark-effect halfwidths measured with shock tube and predicted by semi-empirical theory.

Ion[a]	n_k^*	$E/\lvert\Delta E\rvert$	Transition array	λ(Å)	w_m ($N_e = 10^{17}$ cm^{-3}) (Å)	$w_{SE}^{(4)}/w_m$
Si II	2.94	6.4	$4s$-$4p$	6347.1 6371.4	1.96 ± 20% 1.93 ± 20%	0.92
Si II	3.60	2.0	$4p$-$5s$	5957.6 5979.9	2.78 ± 15% 2.75 ± 15%	1.01
Si II	3.77	4.8	$4p$-$4d$	5041.0 5056.0	2.53 ± 15% 2.69 ± 15%	0.90
Si II	3.94	4.8	$3d$-$4f$	4128.1 4130.0	1.58 ± 25% 1.60 ± 25%	0.76
Ge II	2.98	7.5	$5s$-$5p$	5893.4 6021.0	2.61 ± 15% 1.64 ± 15%	0.61[b]
Ge II	3.91	59.0	$5p$-$5d$	4815.6 4741.8 4824.1	3.10 ± 15% 2.75 ± 15% 3.10 ± 15%	0.98 (0.75)
Ge II	3.95	59.0	$4d$-$4f$	5131.8 5178.5	2.27 ± 15% 2.42 ± 15%	0.99
Sn II	3.09	38.0	$6s$-$6p$	6844.2	4.2 ± 40%	1.19
Sn II	3.72	33.0	$6p$-$7s$	6760.9	5.5 ± 30%	0.85
Sn II	3.91	11.0	$5d$-$4f$	5798.9 5588.8	4.2 ± 30% 3.8 ± 30%	1.25
Sn II	3.98	11.0	$6p$-$6d$	5562.0 5332.4	5.1 ± 15% 5.3 ± 15%	0.96
Pb II	3.13	1.7	$7s$-$7p$	5608.8	1.96 ± 35%	0.71
Pb II	3.91	5.1	$6d$-$5f$	4245.1 4386.4	1.69 ± 20% 1.72 ± 20%	0.94
Pb II	4.08	5.1	$7p$-$7d$	5544.6 5042.5	3.60 ± 20% 3.84 ± 20%	1.36
Pb II	5.74	2.2	$7p$-$9s$	4152.8	2.34 ± 35%	1.02

[a] References: Data for Si II, Ge II, and Sn II were obtained from Refs. 14, 16, and 17, respectively.

[b] The bracketed ratio value obtains if the λ 5893.4-Å broadening is omitted: reviewers (Ref. 22) have commented on the likelihood of the misclassification of this transition.

with exchange) predictions agree with shock-tube measurements. Migdalek's[44] relativistic predictions in *jj* and intermediate coupling (IC) show agreement with the shock-tube measurements in all but one case.

Stark-effect broadening parameters for eight visible Pb II and Pb I lines are presented in Table VI. Electron densities of the measurements appear in the third column. The line full-widths at half intensity are adjusted to an electron density of 10^{17} cm^{-3}. Approximately 90% of the data were collected in the temperature regime $T = 11\,600 \pm 1000$°K; the data have not been treated to compensate for this slight temperature variation. The slit-corrected Lorentzian width components[20] have been ascribed entirely to broadening by the Stark effect of charged plasma constituents. Van der Waals broadening is neglected,[43] as is resonance broadening.[45]

Table VII compares the Stark widths w_m of Pb II, and of homologous group-IV ions measured in the shock tube, with readily calculatable predictions, w_{SE}, based on semiempirical Gaunt factors[4] and the presumption of *LS* coupling. For three of the Pb transition arrays ($7s$-$7p$, $6d$-$5f$, $7p$-$9s$), measured and semiempirical (SE) widths agree within mutual tolerance. However, for the $7p$-$7d$ array, theory slightly overestimates the observed widths. Although the variables n_k^* (effective principle quantum number of upper levels), $E/\Delta E$ (the ratio of mean plasma thermal energy to energy separation from the nearest level perturbing the emitting level),[4] and w_m span considerable ranges, there are no trends to suggest experimental or theoretical bias. Earlier reviews[4,46] of light ion broadening revealed no trends in w_{SE}/w_m over a similar $E/\Delta E$ domain.

To assess the typical reliability of w_{SE} for predicting heavy-element broadening, we inquire about the mean and standard deviation of the w_{SE}/w_m ratio rejecting as per Jones's[46] extensive review of broadening for lighter ($14 < Z < 20$) first-

ion cases where w_{SE}/w_m is greater than 2.0. For the fifteen transition arrays shown in Table VII, w_{SE}/w_m has a mean of 0.97 and a standard deviation of 18%, which characterization does not differ significantly from applications of the SE method[4] or its refined generalization[46] to lighter ($4 \leq Z \leq 20$) systems.

ACKNOWLEDGMENTS

The authors wish to acknowledge the encouragement and support of Dr. T. D. Wilkerson and Dr. V. Lopardo. This research was supported in part by NASA Grants No. NGR-21-002-007/8 and NSG-7347.

[1]J. Migdalek, J. Quant. Spectrosc. Radiat. Transfer 16, 265 (1976).
[2]L. T. Earls and R. A. Sawer, Phys. Rev. 47, 115 (1935).
[3]W. L. Wiese, M. W. Smith, and B. M. Glennon, *Atomic Transition Probabilities*, Natl. Bur. Stand., Res. Ser. 4 (U.S. GPO, Washington, D.C., 1970), Vol. II; Vol. I (1966).
[4]H. R. Griem, Phys. Rev. 165, 258 (1967).
[5]N. Grevesse, Sol. Phys. 6, 383 (1969).
[6]B. M. Glennon and W. L. Wiese, Natl. Bur. Stand. (U.S.), Misc. Publ. 278 (U.S. GPO, Washington, D.C., 1966).
[7]H. A. Bethe and E. E. Salpeter, *Quantum Mechanics of One- and Two-Electron Atoms* (Springer, Berlin, 1957).
[8]E. U. Condon and G. H. Shortley, *The Theory of Atomic Spectra* (Cambridge University, Cambridge, England, 1963).
[9]E. B. Saloman and W. Happer, Phys. Rev. 144, 7 (1966).
[10]R. L. de Zafra and A. Marshall, Phys. Rev. 170, 28 (1968).
[11]R. Novick, B. W. Perry, and E. B. Saloman, Bull. Am. Phys. Soc. II 9, 625 (1964).
[12]P. T. Cunningham and J. K. Link, J. Opt. Soc. Am. 57, 1000 (1967).
[13]E. B. Saloman, Phys. Rev. 152, 79 (1966).
[14]A. LeSage, S. Sahal-Brechot, and M. H. Miller, Phys. Rev. A 16, 1617 (1977).
[15]M. H. Miller and R. A. Roig, Phys. Rev. A 7, 1208 (1973).
[16]W. W. Jones and M. H. Miller, Phys. Rev. A 10, 1803 (1974).
[17]M. H. Miller and R. D. Bengtson, Phys. Rev. A 20, 499 (1979).
[18]R. D. Bengtson, M. H. Miller, D. W. Koopman, and T. D. Wilkerson, Phys. Rev. A 3, 16 (1971); M. H. Miller, R. A. Roig, and R. D. Bengtson, *ibid.* 4, 1709 (1971); M. H. Miller, T. D. Wilkerson, R. A. Roig, and R. D. Bengtson, *ibid.* 9, 2312 (1974).
[19]M. H. Miller and R. D. Bengtson, Phys. Rev. A 1, 983 (1970); M. H. Miller, R. A. Roig, and G. Moo-Young, *ibid.* 4, 971 (1971).
[20]J. T. Davies and J. M. Vaughan, Astrophys. J. 137, 1302 (1963).
[21]P. Kepple and H. R. Griem, Phys. Rev. 173, 317 (1968).
[22]N. Konjevic and W. L. Wiese, J. Phys. Chem. Ref. Data 5, 259 (1976).
[23]M. H. Miller, University of Maryland Technical Note No. BN-550, 1968 (unpublished).
[24]R. D. Bengtson, M. H. Miller, D. W. Koopman, and T. D. Wilkerson, Phys. Fluids 13, 372 (1970).
[25]S. M. Wood and M. H. Miller, Rev. Sci. Instrum. 41, 1196 (1970).
[26]R. A. Bell, R. D. Bengtson, D. R. Branch, D. M. Gottlieb, and R. A. Roig, University of Maryland Technical Note No. BN-572, 1968 (unpublished).
[27]W. R. S. Garton, W. H. Parkinson, and E. M. Reeves, Proc. Phys. Soc. London 88, 771 (1966); M. H. Miller and R. D. Bengtson, J. Quant. Spectrosc. Radiat. Transfer, 9, 1573 (1969).
[28]A. T. Hattenburg, Appl. Opt. 6, 195 (1967).
[29]D. Stuck and B. Wende, Phys. Rev. A 9, 1 (1974).
[30]C. E. Moore, *Atomic Energy Levels*, Natl. Bur. Stand. (U.S.), Circ. 467 (U.S. GPO, Washington, D.C., 1958), Vol. III.
[31]E. P. Trukhan and L. I. Kiselevskii, Acad. Nav. BSSR (Minsk), Doklady 11, 122 (1967).
[32]C. H. Corliss and W. R. Bozman, Natl. Bur. Stand. (U.S.), Monogr. 53 (1962).
[33]W. A. Brown, Phys. Fluids 9, 1273 (1966).
[34]G. Oertel and L. P. Shomo, Astrophys. J. Suppl. Ser. 16, 175 (1968).
[35]D. R. Bates and A. Damgaard, J. R. Astron. Soc. London 242, 14 (1949).
[36]T. Anderson and A. Lindgard, J. Phys. B 10, 2359 (1977).
[37]M. H. Miller and R. D. Bengtson (unpublished).
[38]H. R. Griem, Phys. Rev. 131, 1170 (1963).
[39]J. Lotrian, Y. Guern, J. Cariou, and A. Johannin-Giles, J. Quan. Spectrosc. Radiat. Transfer 21, 143 (1979).
[40]M. Z. Khokhlov, Akad. Nauk SSSR, Krymskaia Astrofizecheskaia Observatoriia, Izvestiia 29, 131 (1963).
[41]N. P. Penkin and I. Yu. Yu. Slavenas, Opt. Spektrosc. (U.S.S.R.), 15, 83 (1963).
[42]D. L. Lambert, E. A. Mallia, and B. Warner, Mon. Not. R. Soc. London 142, 71 (1969).
[43]G. M. Lawrence, Astrophys. J. 148, 261 (1967).
[44]J. Migdalek, Can. J. Phys. 57, 147 (1979).
[45]H. R. Griem, *Plasma Spectroscopy* (McGraw-Hill, New York, 1964).
[46]W. W. Jones, Phys. Rev. A 7, 1826 (1973).